

8. Mathematical model of supersonic heterogeneous in-flow process on a flat obstacle / Nikitin P. V., Borisov S. A., Dobrovolskiy S. V., Glukhovskaya Yu. I. // Surface. X-ray, synchrotron and neutron studies. 2016. Issue 10. P. 50–55. doi: <https://doi.org/10.7868/s0207352816100164>
9. Gomzin A. V., Mikhailov S. A., Gushchina D. S. Evaluation of the State and Development of Aerial Targets Contemporary and Promising Arms Systems // Russian Aeronautics. Aircraft Equipment. 2008. Issue 4. P. 3–6.
10. Ground of structural decisions of airplane-destroyer on basis of radio-location noticeableness hierarchy / Ukrainec E. A., Kotov A. B., Anipko O. B., Tkachov V. V., Onipchenko P. N. // Nauka i tekhnika Povitrianykh Syl Zbroinykh Syl Ukrainy. 2013. Issue 1. P. 20–26.
11. Su-25T // Wikipedia. URL: <https://uk.wikipedia.org/wiki/Cy-25T>
12. Boeвоe primeneniye i TTH sovetskogo istrebitelya SU-25. URL: <https://militaryarms.ru/voennaya-texnika/aviaciya/boeвоe-prime-neniye-i-ttx-sovetskogo-istrebitelya-su-25/>

*Досліджено завадозахищеність існуючих радіоліній з шумоподібними сигналами та цифровими видами модуляції. Аналіз показує, що застосування таких сигналів в умовах радіоелектронного конфлікту не дозволяє забезпечити необхідний рівень показників завадостійкості та прихованості передавання радіоліній зв'язку. Встановлено, що причиною тому є наявність циклостаціонарності несучого коливання в сигналах з цифровими видами модуляції. Такі властивості спрощують виявлення та пошук сигналів за допомогою спектрально-кореляційних методів сучасних засобів радіоелектронної розвідки противника.*

*Для вирішення цієї проблеми запропоновано застосування нестационарних сигнальних конструкцій із змінною центральною частотою та спектральною щільністю потужності. Розроблено методіку формування таких сигнальних конструкцій на основі процедури ортогоналізації Грама-Шмідта до ансамблю багатокomпонентних ЛЧМ сигналів з керованими спектральними характеристиками.*

*Запропоновано оцінювати різні структури сигнальних конструкцій багатокomпонентного сигналу по фазовим портретам сумарних сигналів в залежності від значень коефіцієнта масштабування. Визначено граничні значення цього коефіцієнта, при яких забезпечується ускладнення структури багатокomпонентного сигналу і запобігається виродження процесу в класичну ЛЧМ.*

*Проведено дослідження зміни ймовірності символної помилки в каналі при використанні багатокomпонентних ортогональних сигнальних конструкцій в залежності від співвідношення сигнал/шум. Це дозволяє оцінити потенційну завадостійкість радіолінії за умови, що співвідношення сигнал/шум визначається за енергетичними показниками радіоканалу та спектральною щільністю шумів природного походження.*

*Структурна прихованість розроблених сигнальних конструкцій оцінювалася за допомогою енергетичного детектора і детектора циклостаціонарності. Встановлено, що при енергетичному детектуванні нестационарні сигнали, як і сигнали з будь-яким іншим видом модуляції, еквівалентні. Проте, при використанні детектора циклостаціонарності ймовірність виявлення нестационарних сигнальних конструкцій зменшується в 2–2,5 рази в порівнянні з іншими видами модуляції сигналів*

*Ключові слова: нестационарні багатокomпонентні сигнальні конструкції, ортогоналізація Грама-Шмідта, циклостаціонарність несучого коливання, структурна прихованість*

UDC 004.056

DOI: 10.15587/1729-4061.2018.151816

## DEVELOPMENT OF THE PROCEDURE FOR FORMING NON-STATIONARY SIGNAL STRUCTURES BASED ON MULTICOMPONENT LFM SIGNALS

**V. Korchinskyi**

Doctor of Technical Sciences, Associate Professor\*

E-mail: [vladkorchin@ukr.net](mailto:vladkorchin@ukr.net)

**M. Hadzhiyev**

Doctor of Technical Sciences,  
Associate Professor\*

**P. Pozdniakov**

PhD

Department of General Military,  
Social and Human Sciences\*\*

**V. Kildishev**

PhD, Associate Professor\*

**V. Hordiichuk**

Scientific and organisational division\*\*

\*Department of Information Security  
and Data Transmission

Odessa National Academy of

Telecommunications named after O. S. Popov  
Kuznechna str., 1, Odessa, Ukraine, 65029

\*\*Naval Institute National University  
“Odessa Maritime Academy”

Hradonachalnytska str., 20, Odessa, Ukraine, 65029

### 1. Introduction

Broadband signals (BBS) are used in communication lines to provide structural and parametric security. Such signals are formed by direct-sequencing spread spectrum

(DSSS) and/or frequency hopping spread spectrum (FHSS) [1, 2]. Various types of digital-frequency modulation (DFM) are used in BBS formation: amplitude, phase, frequency or combined modulation. However, the abovementioned modulation methods have a common disadvantage: cyclo-sta-

tionarity, which makes it possible to realize procedures for detecting and determining signal structures [3–5].

Therefore, development of a procedure for formation of nonstationary signal structures which will complicate detection of such signals is a topical line of study.

## 2. Literature review and problem statement

One of the possible ways of improving transmission security is the use of non-positional timer signals with a variable structure. However, this problem is not solved in full because it is aimed at complicating solely structure of the extended digital signal. Therefore, this line requires further studies [6].

Another option for building high-security communication systems is the use of determinate chaotic oscillations [7]. Unlike the regular structure signals, chaotic oscillations have an extended continuous spectrum and low spectral power density which greatly increases complexity of identification and prediction of carrying oscillation parameters. In addition, the use of direct-chaotic transmission can combat multipath propagation and fading in the communication channel. However, the use of chaotic signals in real systems is limited because of low reproducibility and high oscillation instability.

An intermediate position among monochromatic oscillations and determinate chaotic signals belongs to signals with an additive fractal structure. Such signals are irregular in structure and flexible as to variation of characteristics [8].

Thus, use of aggregate signals with controlled structure in which central frequency,  $f_0$ , and spectral power density,  $s(f)$ , vary in time. Such a task can be solved by means of multicomponent LFM signals.

## 3. The aim and objectives of the study

The study objective was to develop a procedure for formation of nonstationary signal structures on the basis of multicomponent LFM signals. This will make it possible to increase security of operation of radio lines by reducing the cyclo-stationary nature of structure of transmitted signals.

To achieve this objective, the following tasks were solved:

- to study dynamics of variation of the multicomponent signal structure depending on the scaling factor value and apply the Gram-Schmidt orthogonalization to a set of multicomponent LFM signals with controlled spectral characteristics;
- to estimate potential noise immunity of the developed signal structures;
- to conduct a comparative analysis of structural security of the developed signal structures in relation to the time-frequency methods of signal detection.

## 4. Orthogonalization of multicomponent LFM signals based on the Gram-Schmidt procedure

### 4.1. Initial data for development of signal structures

It is known [5, 9, 10] that cyclic autocorrelation function is used to estimate correlation properties of cyclo-stationary signals at different frequency pairs. Therefore, in order to ensure stability of the time-frequency detection methods, the developed signal structures must have a zero spectral correlation function, that is, satisfy the condition:

$$\begin{cases} S_x^\alpha(f) = \lim_{\Delta t \rightarrow \infty} \lim_{T \rightarrow \infty} \frac{1}{\Delta t} \frac{1}{T} \int_{-\Delta t/2}^{\Delta t/2} X_T \left( t, f + \frac{\alpha}{2} \right) X_T^* \left( t, f - \frac{\alpha}{2} \right) dt = 0; \\ X_x(t, f) = \int_{t-T/2}^{t+T/2} x(u) e^{-j2\pi fu} du; \end{cases} \quad (1)$$

where  $X_T(t)$  is the spectral component of the process,  $x(t)$ , which is observed at frequency  $f$  in the band width  $1/T$ . Also, such signal structures should have the following statistical characteristics:

$$\begin{aligned} M\{x(t+T_0)\} &\neq M\{x(t)\}, \\ R_x(t+T_0, \tau) &\neq R_x(t, \tau). \end{aligned} \quad (2)$$

where  $M\{x(t)\}$  is the mean value of the process  $x(t)$  at time interval  $t$ ;  $R_x(t, \tau)$  is an autocorrelation function.

LFM signal is used as an initial signal for formation of signal structures:

$$U_0(t) = U_0 \cdot \cos(2 \cdot \pi \cdot f_0 \cdot t + 0.5 \cdot h \cdot t^2 + \phi_0), \quad (3)$$

where  $f_0 = 0.5(f_1 + f_2)$  is average signal frequency;  $t$  is the current time;  $f_1, f_2$  are lower and upper spectrum frequencies;  $h = 2\pi(f_2 - f_1)\tau_0^{-1}$  is frequency change rate;  $U_0, \tau_0, \phi_0$  are amplitude, duration and initial phase of the signal, respectively.

### 4.2. Studying the properties of multicomponent LFM signals as nonstationary signals

Structure of a multicomponent LFM signal depends on the zero (reference) oscillation form and the scaling factor  $k$  which is a quantitative measure of scale invariance of a couple of parameters of LFM oscillations being parts of the formed signal. It is worth noting that multicomponent LFM signals feature a hyperbolic connection between parameters. At the same time, there is a stretch of parameters in one direction (in the case considered, this is the rate of frequency change,  $hk^n$ ) and compression in another direction (decrease in amplitudes of the LFM signal components,  $U_0 k^{-n}$ ). Stretch results in stochasticization but compression is necessary in order that trajectories of the LFM signal components remained in a limited region of the phase space [11, 12].

The considered laws and an expression for classical LFM oscillations make it possible to reduce mathematical expression of a multicomponent signal to the form:

$$U(t) = \sum_{n=0}^{N-1} U_0 \cdot k^{-n} \cdot \cos(2 \cdot \pi \cdot f_0 \cdot t + 0.5 \cdot h \cdot k^n \cdot t^2 + \phi_0), \quad (4)$$

where  $U_0$  is the amplitude of zero (reference) LFM oscillation;  $n, N$  are number and quantity of LFM oscillations involved in formation of a multicomponent signal. Fig. 1, 2 show respectively (in a time domain) a reference LFM oscillation and a multicomponent signal obtained at dimensionless amplitudes  $U_0=1$  and  $U_1=1.75$ ; frequency deviation  $\Delta f=f_2-f_1=8$ ; factor  $k=2$  and signal duration  $\tau_0=2$ . Current time  $t$  was taken in an interval  $[0, 1]$ . The signal (Fig. 1) is a sum of a reference and two homeomorphic (similar) LFM oscillations ( $n=0, 1, 2$  are the component numbers). It can be seen from Fig. 1 and 2 that the multicomponent signal significantly differs from the reference LFM oscillation. Physically, this irregularity is determined by mutual influence (interaction) of the LFM oscillations that are parts of the multicomponent signal.

The degree of irregularity of the multicomponent signal can be visually analyzed and estimated by the phase por-

traits given in Fig. 3, 4. They show behavior of the depicted point in the phase plane. Phase portrait of a classical LFM oscillation with amplitude  $U_1=1.75$  is shown for comparison in Fig. 3. Scatter of phase trajectories (Fig. 4) and their inverse return to the attractor (the attracting set) visually characterizes influence of interaction of all components of LFM oscillations and, as a consequence, the degree of irregularity of the multicomponent signal. Construction of a phase portrait (PP) of signals requires knowledge of derivative (differential) of the function  $U(t)$  [11].

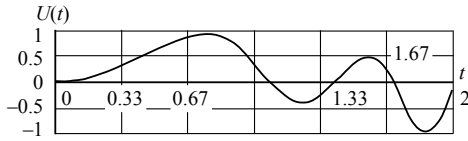


Fig. 1. Time realization of a reference LFM signal

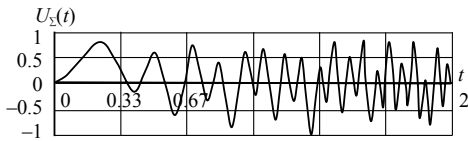


Fig. 2. Time realization of a multicomponent signal

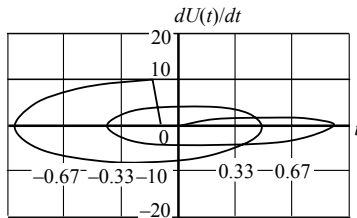


Fig. 3. Time realization of the phase portrait of a reference LFM signal

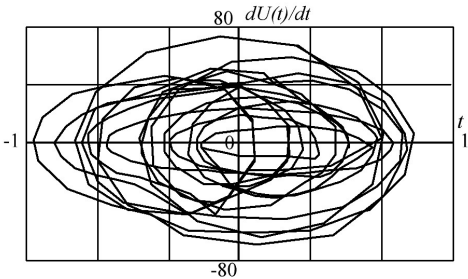


Fig. 4. Time realization of the phase portrait of a multicomponent signal

Next, depict LFM oscillation and a multicomponent signal in a spectral form using the Fourier transform:

$$S(f) = U_1 \cdot \left| \int_{-0.5\tau}^{0.5\tau} e^{j(2\pi(f_0-f)t + 0.5kt^2)} dt \right|; \quad (5)$$

$$S_{\Sigma}(f) = \sum_{n=0}^{N-1} \frac{U_0}{k^n} \cdot \left| \int_{-0.5\tau}^{0.5\tau} e^{j(2\pi(f_0-f)t + 0.5kt^2)} dt \right|. \quad (6)$$

Fig. 5, 6 show the spectra obtained in accordance with formulas (5) and (6). It follows from comparative analysis of the spectra that the multicomponent signal has a continuous extended spectrum in comparison with the classical LFM spectrum. This extension is determined by the influence

of homeomorphic signal components which have spectrum wider than the reference oscillation. The multicomponent signal spectrum is frequency-shifted spectra of LFM oscillations addition of which is determined by the ratio set by the initial model of the multicomponent signal. With an increase in the number of components, the amplitude spectrum is further deformed and the frequency band occupied by the signal extends.

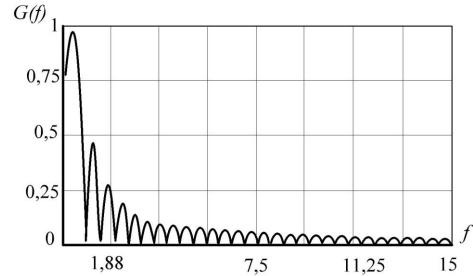


Fig. 5. The reference LFM signal spectrum

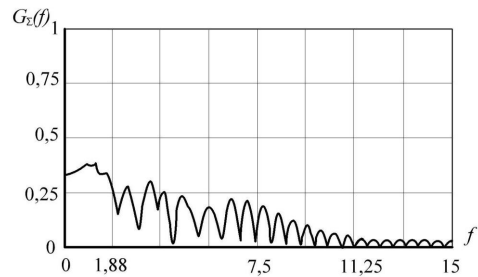


Fig. 6. The multicomponent signal spectrum

Thus, the extended continuous spectrum confirms quasi-randomness of the generated signal. At the same time, the deterministic process of formation using a pseudorandom set of linearly independent multicomponent signals enables obtaining of a plurality of signals with different spectral densities.

Dynamics of the multicomponent signal variation was studied depending on value of the variable scaling factor  $k$  and number of the signal components,  $N=5$ . Analysis of phase portraits of the summed signals has given grounds to conclude that a significant complication of the signal structure begins to occur at the scale factor  $k=1.4$ . Further increase in  $k$  leads to an even more complicated signal. However, with achievement of  $k=2.6$  and its further growth, structure of both the signal and its phase portrait change very weakly. This is due to the fact that amplitudes of the signal components are small when their numbers grow and  $k$  values are significant, so they make a small contribution to the structure of the summed signal. In other words, degeneration of the signal into classical LFM takes place. Thus, it is expedient to choose value of the scaling factor  $k \approx 1.4$  to 2.6 for formation of a summed signal with a rather irregular structure.

Analysis of time realizations and phase portraits of the summed signal with different quantities of components at a fixed value of  $k$  makes it possible to conclude that structural complexity of the signal is mainly determined by its first three components. This is because of insignificant amplitudes of the signal constituents with numbers higher than three. When analyzing time realizations and phase portraits of additive signals,  $N=3$ , it can be concluded that structural

complexity of the signal is determined by the first four components.

**4. 3. Formation of orthogonal signal structures**

Since it is practically impossible to form an infinite series of the function taken in the initial signal model, multicomponent signal structures were studied based on a limited number of components of the initial function. Analysis has shown that to form signal structures, it is appropriate most of all to use an additive set of four components. Dimension of the multicomponent LFM space corresponds to the number of scale factors,  $k_M$ . Taking into account the foregoing, it is possible to form the  $M$ -th alphabet of nonstationary signals:

$$\begin{cases} U_1(t) = \sum_{n=0}^3 U_0 \cdot k_1^{-n} \cdot \cos(2 \cdot \pi \cdot f_0 \cdot t + 0,5 \cdot h \cdot k_1^n \cdot t^2 + \phi_0), \\ U_M(t) = \sum_{n=0}^3 U_0 \cdot k_M^{-n} \cdot \cos(2 \cdot \pi \cdot f_0 \cdot t + 0,5 \cdot h \cdot k_M^n \cdot t^2 + \phi_0). \end{cases} \quad (7)$$

An additional growth of the signal space dimension is possible at the expense of loss of scale invariance of the latter. In this case, dimension of the set of signal structures is  $(N-1)^{k_M}$ :

$$\begin{cases} U_1(t) = \sum_{n=0}^3 U_0 \cdot (k_1 \cdot \xi_j \bmod(k_M))^{-n} \times \\ \times \cos(2 \cdot \pi \cdot f_0 \cdot t + 0,5 \cdot h \cdot (k_1 \cdot \xi_j \bmod(k_M))^n \cdot t^2 + \phi_0), \\ U_M(t) = \sum_{n=0}^3 U_0 \cdot (k_M \cdot \xi_j \bmod(k_M))^{-n} \times \\ \times \cos(2 \cdot \pi \cdot f_0 \cdot t + 0,5 \cdot h \cdot (k_M \cdot \xi_j \bmod(k_M))^n \cdot t^2 + \phi_0), \end{cases} \quad (8)$$

where  $\xi_{j+1} = |\zeta_j - M|$  if  $\xi_j > M$ .

As a result of such construction of (8), frequency arrangement in a series of the initial function differs from geometric progression. However, the insignificant difference in scaling factors supposes quasi-stationarity of the process at certain intervals of observation time. This leads to appearance of phase relations between different signal frequencies and can be used to obtain estimates of the spectral correlation function in corresponding frequency coordinates [12].

In order to eliminate this disadvantage, ensembles of mutually orthogonal multicomponent signals obtained from the  $m$ -dimensional orthonormal basis are proposed. Encoding of the set of information characters is made using linear combinations of orthogonal non-stationary signals. By definition [13], if the random process  $x(t)$  with a finite mathematical expectation  $\mathbf{M}\{x(t)\}$  and continuous correlation function  $R_{xx}(t_1, t_2)$  is set in a closed interval  $[a; b]$ , then there is a complete orthonormal system of functions  $\{u_k(t)\}$  such that

$$x(t) = \sum_{k=1}^{\infty} c_k u_k(t), \quad c_k = \int_a^b \overline{u_k(t)} x(t) dt, \quad (k = 1, 2, \dots), \quad (9)$$

where integrals and a series coincide at a mean value.

Thus, the random process at the output of the radio transmitter can be represented by a set of random factors  $\{c_k\}$ . In particular, there exists a complete orthonormal system  $u_k(t) \equiv \psi_k(t)$  such that all quantities  $c_k$  are uncorrelated standard random quantities.

To obtain a set consisting of  $m$  orthogonal signals, consider  $n$ -dimensional space  $R^n$ . Any point  $\mathbf{p}$  of this space can be represented by an  $n$ -dimensional vector which is a linear sum of the set of orthogonal basis vectors,  $\mathbf{u}_i$ :

$$\mathbf{p} = p_1 \mathbf{u}_1 + p_2 \mathbf{u}_2 + p_3 \mathbf{u}_3 + \dots + p_n \mathbf{u}_n, \quad (10)$$

where  $\mathbf{u}_i \in R^n$ ;  $i \in [1, m]$ ;  $p_i \forall i \in [1, m]$  are valid factors.

Consider a subset consisting of  $m$  basis vectors described by an  $m$ -dimensional subspace within the  $n$ -dimensional space  $R^n$ . A series of vectors describing some hyperspace  $s$  within an  $m$ -dimensional subspace can be represented as:

$$s = c_1 \mathbf{u}_1 + c_2 \mathbf{u}_2 + c_3 \mathbf{u}_3 + \dots + c_m \mathbf{u}_m, \quad s \in R^n \text{ at } n \geq m. \quad (11)$$

Real vectors  $u_i$  can be derived from real-valued functions  $U_i(t)$  as follows. Let  $\mathbf{u}_i = [u_{i1} \dots u_{in}]^T$  and  $U_{ji} = U_i((j-1)T + t_i)$  where  $j \in [1, n]$ ,  $i \in [1, M]$ ,  $t_i$  is the current sampling time at the point of each vector and  $T$  is sampling period. For convenience, write it as matrix  $\mathbf{U} = [\mathbf{u}_1 \dots \mathbf{u}_M]$  where  $U \in R^{nM}$ . In practice, the signal  $\mathbf{u}_i$  vector can be generated by discretization of the real-valued function  $U_i(t)$ . Thus, the problem is reduced to constructing a set of real values of orthogonal vectors  $\mathbf{u}_i \in R^n$  (where  $i \in [1, M]$ ) capable of generating a set of orthogonal functions in real time in the interval  $U_i \forall i \in [1, M]$ ,  $t \in [0, nT]$ . A set of such functions can be obtained using the Gram-Schmidt orthogonalization procedure for a system consisting of  $M$  linearly independent vectors. It should be noted that correspondence of the value of dimension  $n$  to restriction  $n \geq M$  is the mandatory condition for constructing an orthonormal system with  $M$  linearly independent signals taken from the orthogonal basis of the functions  $U_i \forall i \in [1, M]$ .

The Gram-Schmidt orthogonalization procedure for an ensemble of signals  $\{U_i(t), i=1, 2, \dots, M\}$  of duration  $\tau_c$  with energy  $\{E_i, i=1, 2, \dots, M\}$  can be represented as follows [13]:

$$\begin{aligned} y_1(nT) &= U_1(nT), \\ u_1(nT) &= \frac{y_1(nT)}{\sqrt{E_1}}, \\ y_M(nT) &= U_M(nT) - \sum_{i=1}^{M-1} \frac{\langle u_i(nT), U_M(nT) \rangle}{\langle u_i(nT), u_i(nT) \rangle} u_i(nT), \\ u_M(nT) &= \frac{y_M(nT)}{\sqrt{E_M}}. \end{aligned} \quad (12)$$

A message transmitted in radio lines is encoded using linear combinations of orthogonal functions:

$$s(t) = c_1 u_1(t) + c_2 u_2(t) + c_3 u_3(t) + \dots + c_M u_M(t), \quad (13)$$

or in a shorter vector representation:

$$s(t) = \mathbf{u}^T(t) \mathbf{c}, \quad \mathbf{u}^T(t) = [u_1(t), u_2(t), u_3(t), \dots, u_M(t)], \quad (14)$$

where  $\mathbf{u}^T$  is the orthonormal system of vectors;  $\mathbf{c}^T(t) = [c_1, c_2, c_3, \dots, c_M]$  is a linear combination of message characters.

In the process of receiving information symbols, receiver of the radio line determines factors of each orthogonal component by computing  $M$  correlation integrals:

$$c_i = \frac{1}{PT} \int_0^T s(t) u_i(t) dt \quad \forall i \in [1, M], \quad (15)$$

$$P_i = \frac{1}{T} \int_0^T u_i^2(t) dt, \quad (16)$$

which can be represented in an equivalent vector representation with taking into account (15) and (16) as follows:

$$c = \frac{\int_0^T u(t)s(t) dt}{\int_0^T u(t)u^T(t) dt}. \quad (17)$$

Expression (17) is valid for any orthogonal set of signals. Distinctive feature of this system consists in that signals can be transmitted sequentially via a separate channel and simultaneously via all channels. The system throughput will be determined by dimension of the ensemble of orthogonal signal structures. Fig. 7 shows a diagram of an orthogonal multi-component signal shaper.

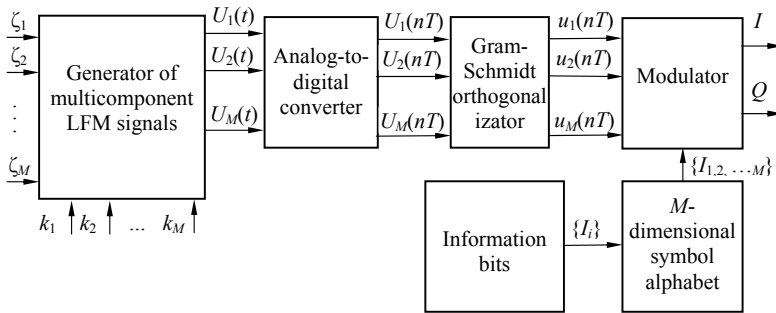


Fig. 7. Block diagram of a shaper of multi-component orthogonal signal structures

Generator of multicomponent signals generates a set consisting of  $M$  additive LFM signals. Each signal consists of a set of components obtained from initial oscillation at different scaling factors  $k$ . Choice of components of the summed oscillation is made according to the pseudorandom law with the help of a control parameter  $\xi_j$ . Digitized signal samples are orthogonalized using the Gram Schmidt procedure and arrive at the modulator.

### 5. Estimation of potential noise immunity of radio lines

Let us calculate potential noise immunity of radio lines as a probability that the system detector performs an optimal signal receival. For orthogonal signals of equal energy, optimal detector will select a signal that will have the greatest correlation with the received signal  $s$  and each of  $M$  possible signal vectors  $\{u_m\}$ , that is:

$$C(s, u_m) = s \cdot u_m = \sum_{k=1}^M s_k \cdot u_{mk}, \quad (18)$$

$m = 1, 2, \dots, M.$

Since the probability density functions at the output of correlators,  $\{r_m\}$ , are statistically independent, the common probability density will be determined by the product  $M-1$  of the proper probabilities of the form:

$$p(n_m < r_1 | r_1) = \int_{-\infty}^{r_1} p_{r_m}(x_m) dx_m = \frac{1}{\sqrt{2\pi}} \int_{-\infty}^{r_1 \sqrt{2/N_0}} e^{-\frac{x^2}{2}} dx. \quad (19)$$

These probabilities are the same for  $m=2, 3, \dots, M$ , that is, the cumulative probability (the probability of correct receival) is defined as:

$$P_c = \int_{-\infty}^{\infty} \left( \frac{1}{\sqrt{2\pi}} \int_{-\infty}^{r_1 \sqrt{2/N_0}} e^{-\frac{x^2}{2}} dx \right)^{M-1} p(r_1) dr_1. \quad (20)$$

Thus, probability of a character error in a radio channel can be defined as in [14]:

$$P_M = 1 - P_c = \frac{1}{\sqrt{2\pi}} \int_{-\infty}^{\infty} \left[ 1 - \left( \frac{1}{\sqrt{2\pi}} \int_{-\infty}^y e^{-\frac{x^2}{2}} dx \right)^{M-1} \right] e^{-\frac{1}{2} \left( y - \sqrt{\frac{2E_s}{N_0}} \right)^2} dy. \quad (21)$$

Fig. 8 presents results of numerical simulation of a character error from the signal-to-noise ratio (S/N).

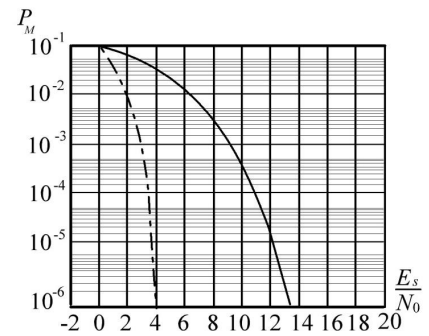


Fig. 8. Noise immunity of radio communication lines with the use of developed signal structures

The firm curve shows the lower limit for probability of a character error when two signal structures are used. The dashed line represents maximum achievable (in terms of practical implementation) value of probability of a character error when using 1024 orthogonal signal structures. Expression (21) allows one to estimate noise immunity of the radio line in idealized conditions when the S/N is completely determined by energy indicators of the radio channel,  $E_s$ , and the spectral density of the noise of natural origin  $N_0$ . In most practical applications, it is advisable to consider both noise immunity and security of radio lines [15].

### 6. Analysis of structural security of the developed signal structures and signals with digital modulation types in relation to the time-and-frequency methods of signal detection

The radio line security can be quantified by the probability of signal detection. The algorithm of searching for the spectral harmonic corresponding to the symbol frequency can be described as follows. The band which is determined by the formula (22) is only taken for analysis in the signal spectrum at the output of a nonlinear operator. A spectral component with maximum amplitude and an extreme right harmonic whose amplitude exceeds  $0.25S_{max}$  are sought in this band. The value of the latter frequency is taken as an estimate of symbol frequency.

Figs. 9, 10 show dependence of probability of correct recognition,  $P_{rec}$  16-PSK and 128-QAM using common phase constellation and combination of the common phase constellation

with its squared variant. It can be concluded from analysis of the dependences depicted in Fig. 9, 10 that application of exponentiated variants of phase constellations can significantly improve probability of correct recognition of modulation type in a range of low S/N values. For example, probability of correct recognition of 128-QAM at S/N 8dB increases from 0 to 0.98.

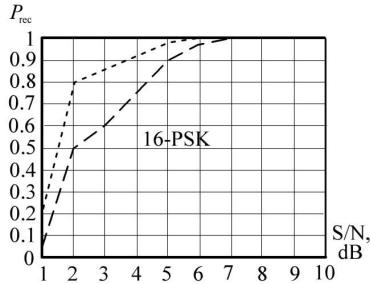


Fig. 9. Probability of recognition of signals from 16-PSK using a squared constellation: for combined phase constellations (- - -); for ordinary phase constellations (- - -)

Calculation of the spectrum width is realized in the following way. Amplitude-frequency spectrum is calculated by means of a fast Fourier transform. An example of such a spectrum for a signal with an eight-fold PSK is shown in Fig. 11. To reduce influence of fluctuations of spectral harmonics on accuracy of the spectral width measurement, arithmetic averaging of amplitudes of neighboring harmonics was used:

$$S_c(kF) = \sum_{n=k}^{k+N} \frac{S(nF)}{N}, \tag{22}$$

where  $N$  is the number of read-outs taken for averaging. An example of the averaged spectrum is shown in Fig. 12.

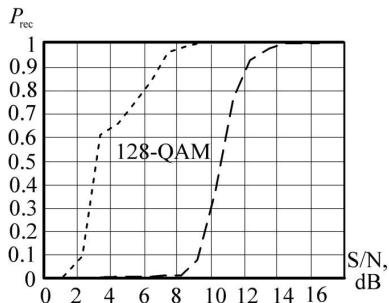


Fig. 10. Probability of 128-QAM signal recognition using a squared constellation: for combined phase constellations (- - -); for ordinary phase constellations (- - -)

Spectrum width,  $\Delta f_{c0}$ , is calculated as a difference in frequencies of spectral components of the smoothed spectrum that exceed the value of the set threshold,  $S_p$ , to the right and left of the central value of frequency  $f_{c0}$  calculated by the following expression:

$$f_{c0} = \frac{\sum_i f_i S_c(f_i)}{\sum_i S_c(f_i)}, \tag{23}$$

where  $S_c(f_i)$  is amplitude of the spectral harmonic corresponding to frequency  $f_i$ .

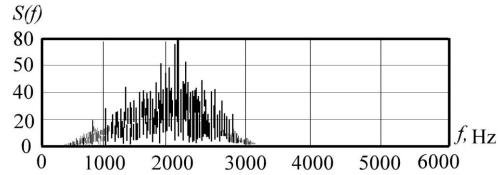


Fig. 11. Initial amplitude-frequency spectrum of the received 8-PSK signal

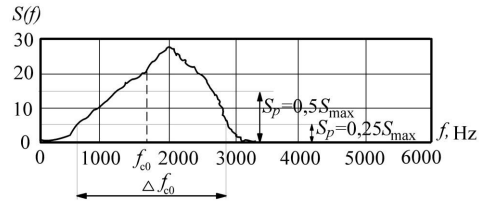


Fig. 12. Averaged amplitude-frequency spectrum of the received 8-PSK signal

The calculated value of the spectrum width,  $\Delta f_{c0}$ , is taken as the central value of frequency of the band of spectral peak search which corresponds to the symbol frequency. The conducted studies with simulated and real signals show that the spectral harmonic corresponding to the symbol frequency is within the frequency band in a vast majority of cases:

$$\Delta f_{c0} - \frac{\Delta f_{c0}}{2} \dots \Delta f_{c0} + \frac{\Delta f_{c0}}{2}. \tag{24}$$

Thus, a harmonic of symbolic frequency will be sought solely within the band defined by expression (24). In most cases, the harmonic corresponding to the symbol frequency has maximum amplitude,  $S_c$ , in the signal spectrum from the output of the nonlinear limiter (Fig. 13). This fact is used for its search in existing algorithms of symbol frequency estimation. This enables analysis and classification of signals, even in the case of low S/N and strong signal distortion. Therefore, application of spectral-correlation analysis methods is most appropriate currently (Fig. 14).

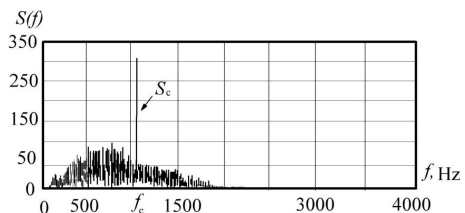


Fig. 13. Initial spectrum of the module of aggregate signal amplitude

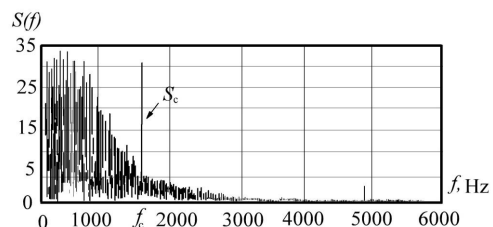


Fig. 14. Spectrum of the module of the aggregate amplitude of the signal distorted by influence of the propagation medium

The performed simulations show that the spectral component of the symbol frequency is the extreme right harmon-

ic in the spectrum of the signal with amplitude greater than  $0.25S_{\max}$  where  $S_{\max}$  is the maximum amplitude in the signal spectrum. The cyclo-stationarity detector can be described in general by the following expressions:

$$M\{s(t_1)\} = \lim_{N \rightarrow \infty} \frac{1}{N} \sum_{k=1}^N s_k(t_1) \quad (27)$$

and

$$R_{ss}(t_1, t_1 + \tau) = \lim_{N \rightarrow \infty} \frac{1}{N} \sum_{k=1}^N s_k(t_1) s_k(t_1 + \tau). \quad (28)$$

Let us analyze spectral correlation functions (Fig. 15, 16) of a classical broadband phase-modulated signal and a non-stationary signal. Obviously, the developed structures qualitatively differ from classical broadband signals. This makes it possible to increase security of information transmission via radio lines on the basis of spectral and correlation analysis of signals.

In the general case, when the process is non-stationary, the values

$$M\{s(t_1)\} = \lim_{N \rightarrow \infty} \frac{1}{N} \sum_{k=1}^N s_k(t_1) \quad (27)$$

and

$$R_{ss}(t_1, t_1 + \tau) = \lim_{N \rightarrow \infty} \frac{1}{N} \sum_{k=1}^N s_k(t_1) s_k(t_1 + \tau) \quad (28)$$

are not invariant with respect to the transfer of moment  $t_1$  [16]. For any  $t=t_1$ , probability density of such a process  $p(s, t_1)$  is described by the expression

$$p(s, t_1) = \lim_{\Delta \rightarrow 0} \frac{P[s < s(t_1) < s + \Delta s]}{\Delta s}. \quad (29)$$

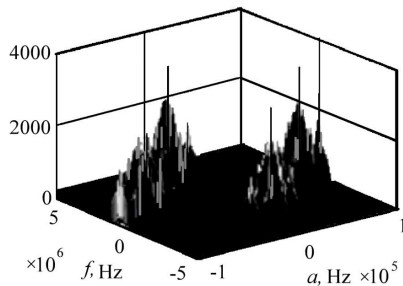


Fig. 15. Spectral correlation function of a binary PSK signal

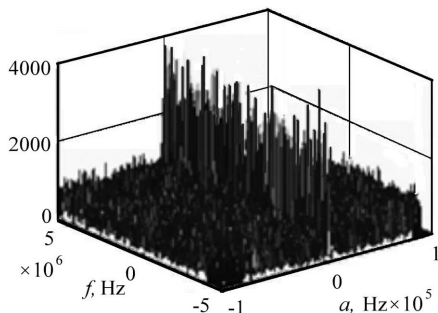


Fig. 16. Spectral correlation function of non-stationary signal

Let us determine signal at the output of the radio line transmitter through a Gaussian stationary process  $n(t)$  with a zero mathematical expectation and a deltoid correlation function

$$s(t) = \int_0^t n(\tau) d\tau, \quad (30)$$

$$E\{n(t)\} = 0, \quad (31)$$

$$R(t_2 - t_1) = \left(\frac{N}{2}\right) \delta(t_2 - t_1). \quad (32)$$

According to [16], if the initial process is expressed through the Gaussian by means of a linear transformation, then it is Gaussian as well. According to (31), mathematical expectation, dispersion and correlation function of this process are described as follows:

$$E\{s(t)\} = 0, \quad (33)$$

$$D_s(t) = \int_0^t \int_0^t E\{n(\tau_1)n(\tau_2)\} d\tau_1 d\tau_2 = \frac{N}{2} t, \quad (34)$$

$$R(t_1, t_2) = \int_{t_0}^{t_1} \int_{t_0}^{t_2} E\{n(\tau_1)n(\tau_2)\} d\tau_1 d\tau_2 = \frac{N}{2} (t_1, t_2). \quad (35)$$

Define properties of increments in the intervals that do not intersect ( $t_3 > t_2 > t_1$ ) from an it follows from obvious equality

$$s(t_2) - s(t_1) = \int_{t_1}^{t_2} n(\tau) d\tau, \quad (36)$$

that the mathematical expectation is zero and the dispersion of increments is proportional to the difference between the moments of time:

$$M\{[s(t_2) - s(t_1)]^2\} = \frac{N}{2} (t_2 - t_1), \quad t_2 > t_1. \quad (37)$$

Mutual correlation of the function of increments using (35) is defined as

$$\begin{aligned} M\{[s(t_3) - s(t_2)][s(t_2) - s(t_1)]\} &= \\ &= R_s(t_3, t_2) - R_s(t_2, t_2) - R_s(t_3, t_1) + R_s(t_2, t_1) = 0. \end{aligned} \quad (38)$$

Thus, the process increments,  $s(t)$  in non-overlapping time intervals are uncorrelated, and given normal distribution, they are independent which should have been proved. In addition, the process increments can be called stationary since their mathematical expectation is zero and dispersion is proportional to the difference between the time moments. The following formula is a direct consequence of these features:

$$\lim_{\Delta \rightarrow 0} S_m = \lim_{\Delta \rightarrow 0} \sum_{i=0}^{m-1} [s(t_2) - s(t_1)]^2 = \frac{N(t - t_0)}{2}, \quad (39)$$

where  $t_0 < t_1 < \dots < t_m < t$ ,  $\Delta = \max(t_{i-1} - t_i)$ .

The convergence of the sequence of random sums to the left and the non-random variable to the right is interpreted as convergence by probability.

This confirms the assumption that a multicomponent orthonormal signal is a Gaussian non-stationary process with zero mathematical expectation and a dispersion proportional to time. Realizations of the process are increasingly scattered and non-reproducible with the course of time (Fig. 17, 18).

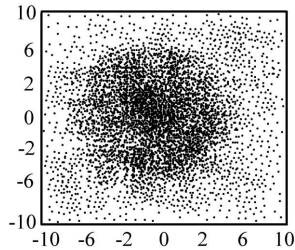


Fig. 17. Vector diagram of multicomponent orthogonal signal structures (10,000 realizations)

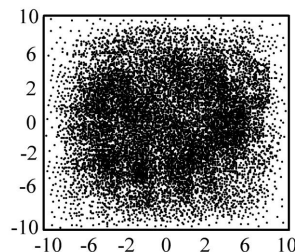


Fig. 18. Vector diagram of multicomponent orthogonal signal structures (50,000 realizations)

Signal constellations from the computer are shown for comparison in Fig. 19, 20.

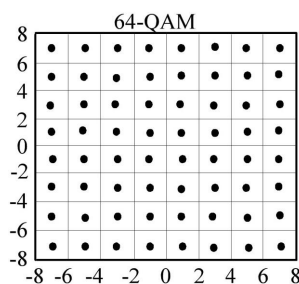


Fig. 19. Vector diagrams of signals from 64-QAM

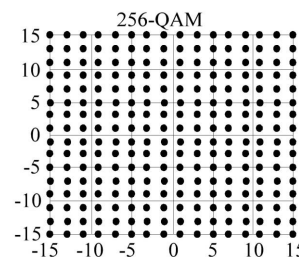


Fig. 20. Vector diagrams of signals from 256-QAM

To establish structural security of the developed signal structures, expressions describing the energy detector and the cyclo-stationarity detector are used. In the case of detecting a single spectral component using a cyclo-stationarity detector, the following expressions can be used:

$$z_{sc}(N) = \int_{\frac{f_s}{2}}^{\frac{f_s}{2}} S_x^\alpha(f) S_y^{\alpha*}(f) df, \tag{40}$$

$$d = \frac{E(z_{sc} | H_1) - E(z_{sc} | H_0)}{\sqrt{Var(z_{sc} | H_0)}}, \tag{41}$$

where  $Var()$  is the mean square deviation. For energy detection of the signal:

$$d(0) \sim \frac{d_0(0) SNR_{in} \sqrt{N}}{\sqrt{1 + \sigma_N \left(1 + \frac{3}{2} N\right)}}. \tag{42}$$

Characteristics of detecting the developed nonstationary signal structures are shown in Fig. 21.

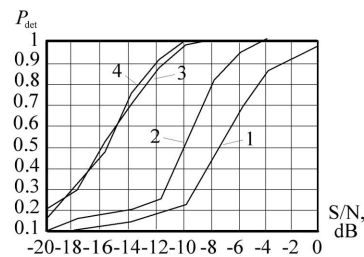


Fig. 21. Dependence of the probability of detecting orthogonal signals and developed signal structures on S/N by means of the energy detector and the cyclo-stationarity detector (probability of false alarm,  $P_{fa}=0.1$ ): developed SK SD (1); orthogonal SK SD (2); developed SK ED (3); orthogonal SK ED (4)

It follows from analysis of dependences shown in Fig. 21 that in the case of energy detection, nonstationary signals as well as signals with any other type of modulation are equivalent. It can also be seen that when using the cyclo-stationarity detector, probability of detecting non-stationary signal structures is 2–2.5 times lower compared to other types of signal modulation.

### 7. Discussion of the results obtained in the study and development of non-stationary signal structures

The obtained results enable growth of transmission security in communication radio lines by means of non-stationary signal structures in comparison with traditional broadband signals as to spectral and correlation analysis. This makes it possible to ensure transmission immunity to an organized noise. This is due to the fact that spectrum of the proposed multicomponent signal is continuously extended in comparison with the spectrum of classical LFM oscillation.

The study of dynamics of the multicomponent signal variation depending on value of the variable scaling factor,  $k$ , and number of the signal components  $N=5$  has established limit values of these indicators. Significant complication of the signal structure begins to manifest itself at the scaling factor  $k=1.4$  and decelerates at  $k=2.6$ . Thus, to form a multicomponent signal, it is expedient to choose value of the scaling factor  $k \approx 1.4-2.6$ . This is of particular importance in development of modern military radio communication lines.

It was proposed to provide required level of noise immunity through formation of non-stationary orthogonal signals with minimal mutual correlation. This is ensured by applying the Gram-Schmidt orthonormalization procedure to a series of multicomponent LFM signals with controlled spectral characteristics.

To estimate structural security of the developed signal structures, an analysis was made taking into account operation of the energy detector and the cyclo-stationarity detector. It was proved that in the case of energy detection, nonstationary signals and signals with any other type of modulation are equivalent. However, when using the cyclo-stationarity detector, probability of detecting non-stationary signal structures is 2–2.5 times lower compared to other types of signal modulation.

The proposed methods of formation of nonstationary signals are the continuation of the study on construction of jam-resistant communication systems with noise-type signals designed to work in conditions of radio-electronic conflict. In the proposed embodiment, it is possible to achieve transmission rate of up to 5 Mbit/s, which is acceptable for military radiocommunication systems but not enough for civilian ones. Further development of the study will be advisable in a direction of increasing noise immunity and transmission speed by introducing additional signal processing procedures, e.g. preliminary

noise immune encoding, change of the orthogonalization procedure, etc.

---

## 8. Conclusions

---

1. It was found that complexity of irregular structure of a multi-component LFM signal is ensured at values of the scaling factor  $k \approx 1.4$ – $2.6$  and the number of the signal structure components  $N=5$ . Complexity rate of the signal structure is slowing down at  $k > 2.6$ . Orthogonalization of multicomponent LFM signals based on the Gram-Schmidt procedure is aimed at increasing transmission security through reduction of cyclo-stationarity in signal structures.

2. The study has revealed that potential noise immunity of the radio line worsens with growth of the ensemble of non-stationary signal structures being used. This is explained by the fact that the energy distance between the signal structures of the ensemble decreases.

3. It was shown that the use of non-stationary signal structures ensures growth of structural security of signals in comparison with traditional broadband signals as to spectral and correlation analysis. When using a cyclo-stationarity detector, probability of detecting non-stationary signal structures is 2–2.5 times lower compared to other types of signal modulation.

---

## References

1. Korchinskiy V. Method of increase of reserve of transfer by timer signals in communication systems with code division of channels // *Visnyk Skhidnoukrainskoho natsionalnoho universytetu imeni Volodymyra Dalia*. 2013. Issue 15. P. 93–99.
2. Kandyryn N. P. Cifrovye metody formirovaniya signalov v RLS s izmenyayushcheysoya nesushchey chastotoy // *Systemy ozbroiennia i viyskova tekhnika*. 2014. Issue 3 (39). P. 100–107.
3. Aksenov V. V. Ocenivanie signal'no pomekhovoy obstanovki radioreleynogo kanala peredachi dannyh // *Spektekhnika i svyaz'*. 2013. Issue 3. P. 45–48.
4. Aksenov V. V., Pavlov V. I. Application of bayesian approach to evaluate the signal-interference situation in information transfer channel of processing communication system // *Vestnik Tambovskogo gosudarstvennogo tekhnicheskogo universiteta*. 2013. Vol. 19, Issue 2. P. 284–290.
5. Kuzyk A. Spectral and correlation analysis of signals with continuous and discrete frequency modulation // *Visnyk Natsionalnoho universytetu "Lvivska politekhnika"*. Radioelektronika ta telekomunikatsiyi. 2016. Issue 849. P. 31–44.
6. Assessing the Impact of the Noise on the Throughput Communication Channel with Timing Signals / Zakharchenko N. V., Korchinskiy V. V., Radzimovsky B. K., Bektursunov D. N., Gorokhov Y. S. // *Eastern European Scientific Journal*. 2015. Issue 4. P. 209–214.
7. Stealth of transmission in communication systems with chaotic signals / Zakharchenko M. V., Horokhov S. M., Korchynskii V. V., Radzymovskii B. K. // *Vymiriuvalna ta obchysliuvalna tekhnika v tehnolohichnykh protsesakh*. 2013. Issue 3. P. 161–164.
8. Korchinskiy V. V. Model' shumovogo signala dlya peredachi konfidencial'noy informacii // *Vestnik NTU «KhPI»*. 2013. Issue 11 (985). P. 90–95.
9. Mathematical model of intercept single signal hop transmitter with FHSS / Yerokhin V., Roma O., Vasylenko S., Bezdrabko D. // *Visnyk Natsionalnoho tekhnichnoho universytetu Ukrainy "Kyivskiy politekhnichnyi instytut"*. Seriya: Radiotekhnika. Radioaparatabuduvannia. 2016. Issue 64. P. 75–85.
10. Sha'ameri A. Z., Kanaa A. Robust multiple channel scanning and detection of low probability of intercept (LPI) communication signals // *Defense S&T technical bulletin*. 2016. Vol. 9, Issue 1. P. 1–17.
11. Domatyrko D. G., Panychev S. N., Churakov P. P. Research LFM signals in models of nonlinear radar founding of objects // *Vestnik Voronezhskogo gosudarstvennogo tekhnicheskogo universiteta*. 2014. Vol. 10, Issue 5. P. 21–25.
12. Kandyryn N. P. Forming of wideband LFM signals and transfer of them method of direct digital synthesis in range GSE. Part 1. Forming of the precision LFM signals of DDS by synthesizers // *Systemy obrobky informatsiyi*. 2016. Issue 3. P. 64–68.
13. Piskova A. V., Menshchikov A. A., Korobeynikov A. G. Use of Gram-Schmidt orthogonalization in the lattice basis reduction algorithm for security protocol // *Voprosy kiberbezopasnosti*. 2016. Issue 1 (14). P. 47–52.
14. Shtompel M. A. Functional representation of linear error correcting codes // *Nauka i tekhnika Povitrianykh Syl Zbroinykh Syl Ukrainy*. 2017. Issue 1. P. 120–122. doi: <https://doi.org/10.30748/nitps.2017.26.24>
15. Shtompel M. Development trends of methods of error-correcting coding information in telecommunications // *Zbirnyk naukovykh prats Kharkivskoho natsionalnoho universytetu Povitrianykh Syl*. 2017. Issue 1. P. 35–37.
16. Metody modelirovaniya sluchaynykh processov / Selihov Yu. R., Yurskov S. V., Shuklin A. V., Hamush A. L., Gazarov D. A. // *Molodoy ucheniy*. 2016. Issue 11. P. 467–471.